IC/82/111

INTERNATIONAL CENTRE FOR THEORETICAL PHYSICS

SU(N)-QCD$_2$ MESON EQUATION IN NEXT-TO-LEADING ORDER

M. Durgut

and

N.K. Pak

INTERNATIONAL ATOMIC ENERGY AGENCY

UNITED NATIONS EDUCATIONAL, SCIENTIFIC AND CULTURAL ORGANIZATION

1982 MIRAMARE-TRIESTE

International Atomic Energy Agency
and
United Nations Educational Scientific and Cultural Organization

INTERNATIONAL CENTRE FOR THEORETICAL PHYSICS

SU(N)-QCD$_2$ MESON EQUATION IN NEXT-TO-LEADING ORDER *

M. Durgut** and N.K. Pak**
International Centre for Theoretical Physics, Trieste, Italy.

ABSTRACT

We compute the 1/N corrections to the meson equation in the regular cut-off scheme. We illustrate that although the quark and gluon self-energy and vertex corrections do not vanish explicitly as in the singular cut-off scheme, their contributions to the meson Bethe-Salpeter equation get cancelled within the whole set of contributing diagrams. We also argue that O(1/N) corrections to the meson equation remove the massless boson from the spectrum in accordance with the Coleman theorem.

MIRAMARE - TRIESTE
August 1982

* To be submitted for publication.

** Permanent address: Department of Physics, Middle East Technical University, Ankara, Turkey.

I. INTRODUCTION

The reason why QCD$_2$ is taken to be a serious laboratory is that it exhibits both scaling and confinement [1)-3)].

A rather promising method of computation for the SU(N) gauge theories is to expand them in powers of 1/N. [1)] That 1/N does not suffer from the renormalization problem (that this expansion does not break at short or large distances) makes it a very attractive perturbation scheme. Because the method of summation of Feynman diagrams is non-perturbative in g^2N (where g is the gluon fermion coupling) but is perturbative in 1/N, one sums over all the contribution of the same order in O(1/N). Moreover, in a given order, the infinite set of diagrams involved are characterized by a well-defined topology of quarks and gluons [4)].

As a check of the consistency of the 1/N scheme, it is important to evaluate higher orders in 1/N. One could, for example, worry whether radiative corrections to the gluon and quark propagators and to the gluon-quark vertex may radically alter the properties of the model.

In the planar limit ($N \to \infty$), hadronic bound states acquire real masses and hence are stable [1),2)]. However, in the non-leading order the mass operator gains an imaginary part as well as corrections to its real part [3)]. In that respect, the non-leading corrections may also offer insight into the question of the narrowness of the hadronic widths.

Previously, 1/N corrections to the SU(N)-QCD$_2$ have been studied for the meson-meson scattering problem, and order 1/N terms have been shown to exhibit embryonic Regge behaviour with the crossed channel factorization, signature and exchange degeneracy properties found in the dual Regge amplitudes [5)]. Here our main concern will be the meson bound state spectrum.

The 1/N corrections depend strongly on the infra-red cut-off scheme employed. Indeed the non-renormalization property of the gluon propagator in the λ cut-off scheme follows directly from the confinement mechanism which is automatically implemented in this cut-off scheme [2)]. We have carried out our analysis in the principal value cut-off scheme (also known as the regular cut-off) [3),6)]. This cut-off scheme has the advantage that the theory is totally free of infra-red infinites, although the quark confinement is less transparent. Furthermore, the properties of the gauge non-invariant sector become quite different; for example, the quark propagator has a pole at finite mass [2)].

The non-renormalization properties of the gluon and quark propagators are also very different and more complicated than in the singular cut-off scheme. It follows from our analysis that the quark and gluon self-energy diagrams and vertex corrections do not vanish explicitly in the principal value cut-off scheme, as in the singular cut-off scheme, but they are cancelled within the set of all Feynman diagrams of a given process. This is demonstrated in detail in Sec.IV, where the meson bound state equation is obtained to order 1/N.

The paper is organized as follows. In Sec.II, the planar limit of two-dimensional QCD is reviewed (to make the paper self-contained), with emphasis on the quark-antiquark scattering matrix and the proper quark-antiquark meson vertex, which are extensively used in later sections. In Sec.III, the higher order terms to the quark and gluon operators and to the gluon-quark vertex are computed in O(1/N). By means of the bootstrap equation, the O(1/N) quark mass contribution is shown to be a radiative correction to the quark operator where the exchanged fields are the planar meson bound states. In Sec.IV, the Bethe-Salpeter equation for the meson bound state is evaluated to O(1/N). The non-leading Feynman diagrams of the bound state are explicitly evaluated and their phyiscal significance is discussed. It is also shown how the gluon and quark self-energies and the vertex corrections found in Sec.II, get cancelled within the whole set of those diagrams. In addition to the single loop (worm-hole) correction to the planar limit, which is a s-channel diagram with two intermediate meson states, there are the t-channel meson exchange diagram and the crossed-gluon diagram, which contribute in the equal quark mass limit. The crossed gluon diagram is shown to lead to a t-channel diagram with an intermediate quark-quark bound state when this diagram is considered to all orders in 1/N. In Sec.V, we briefly discuss the status of the massless boson and in view of the results of Sec.IV, argue that the O(1/N) corrections to the meson equation remove it from the spectrum, in conformity with Coleman's theorem [7] that there are no Goldstone bosons in two dimensions.

II. A REVIEW OF THE LEADING ORDER 1/N ANALYSIS OF TWO-DIMENSIONAL YANG-MILLS THEORY

Quantum chromodynamics with SU(N) colour gauge group is defined by the Lagrangian

$$\mathcal{L} = -\tfrac{1}{4} F^a_{\mu\nu} F^{\mu\nu,a} + \bar{\psi}\,(i\not{D} - m)\psi$$

$$F^a_{\mu\nu} = \partial_\mu A^a_\nu - \partial_\nu A^a_\mu + g f^{abc} A^b_\mu A^c_\nu$$

$$D_\mu \psi = \partial_\mu \psi - i g A^a_\mu \frac{\lambda^a}{2} \psi$$

$$a = 1, \ldots, N^2-1 \qquad (2.1)$$

and we have suppressed the flavour indices. The light-cone gauge proves particularly convenient in two dimensions

$$A_- = A^+ = 0 \qquad (2.2)$$

In this gauge $\mathcal{L}$ reduces to the following simple form:

$$\mathcal{L} = \tfrac{1}{2}(\partial_- A^a_+)^2 + \bar{\psi}(i\not{D} - m)\psi + g\,\bar{\psi}\gamma_- \frac{\lambda^a}{2}\psi\, A^a_+ \qquad (2.3)$$

The effective Feynman rules (for which the computations involving γ_+ and γ_- matrices have already been done) corresponding to the Lagrangian in (2.3) are illustrated in Fig.1.

The two-dimensional gauge theories are extermely infra-red divergent, which necessitates the introduction of an infra-red cut-off. Because the gauge invariant quantities are to be free of the infra-red singularities, we can choose the cut-off procedure to suit our purposes best. In this respect, we define the gluon propagator with "principal value prescription" and avoid the infra-red divergence altogether [2),6)]

$$\frac{1}{k_-^2} = \frac{1}{2}\left[\frac{1}{(k_+ + i\varepsilon)^2} + \frac{1}{(k_- - i\varepsilon)^2}\right]$$

The ordinary perturbation theory becomes ineffective in discussing the spectrum and the infra-red properties of the non-Abelian gauge theory and one has to resort to non-perturbation techniques. 't Hooft has developed the large N expansion, where one expands the Green functions in powers of 1/N, keeping g^2N fixed and summing to all orders in g^2N. The dominant diagrams in this expansion, then consists solely of the planar diagrams with quarks at the edges. No fermion loops can occur at the lowest order.

Before we present our analysis of the next-to-leading order corrections in 1/N, let us briefly discuss the planar limit of quark-anti-quark scattering. In the discussion of the $q\text{-}\bar{q}$ scattering and the meson bound state, the central object is the $q\text{-}\bar{q}$ scattering amplitude, given in Fig.2 which satisfies a Bethe-Salpeter equation in the planar limit[1),2)] We define the proper quark-anti-quark meson proper vertex [3)] as

$$\Gamma(x, M^2) = -\frac{g^2}{\pi}\left(N - \frac{1}{N}\right) \int \frac{dy}{(y-x)^2}\, \phi(y, M^2) \qquad (2.4)$$

where $\int$ represents a principal value integral, $x = \frac{p_-}{r_-}$ is the scaled quark momentum; r denotes the meson momentum and the meson mass is $M^2 = 2r_-r_+$. Eq.(2.5) is described diagramatically in Fig.3 where the dotted lines represent the meson state, the crossed blob is the wave function ϕ.

For the x values $1 \geq x \geq 0$, Eq.(2.4) becomes

$$\Gamma(x, M^2) = \left(M^2 - \frac{m_i^2}{x} - \frac{m_j^2}{1-x}\right) \phi(x, M^2) \qquad (2.5)$$

where m_i and m_j are the quark and antiquark masses, respectively.

The leading order scattering amplitude is determined from the Bethe-Salpeter equation in Fig.2

$$T(p,q;r^2) = -\frac{ig^2}{(p-q)^2} + \frac{ig^2}{r_-^2}\left[\frac{g^2}{\pi}\left(N - \frac{1}{N}\right)\right]^{-1} \sum_n \frac{\Gamma_n(p,r_-)\Gamma_n(q,r_-)}{r_-^2 - M_n^2 + i\varepsilon} \qquad (2.6)$$

or

$$T(x,y;r^2) = \frac{ig^2}{r_-^2}\left\{-\frac{1}{(x-y)^2} + \left[\frac{g^2(N-1/N)}{\pi}\right]^{-1} \sum_n \frac{\Gamma_n(x)\Gamma_n(y)}{r_-^2 - M_n^2 + i\varepsilon}\right\} \qquad (2.7)$$

where $x = \frac{p_-}{r_-}$, $y = \frac{q_-}{r_-}$, M_n^2 is the intermediate meson mass. In Fig.4, the diagrams of Eq.(2.7) are shown.

When the quark momenta x,y satisfy the bound state condition $x,y \in O(1)$, it is possible to rearrange the terms in Eq.(2.7) so that the single gluon term disappears. We distinguish the following two cases:

i) $\underline{0 \leq x \leq 1}$

In this case T is decomposed as

$$T(x,y;r^2) = \frac{ig^2}{r_-^2}\left[\frac{g^2}{\pi}\left(N - \frac{1}{N}\right)\right]^{-1} \sum_n \frac{M^2 - m_i^2/x - m_j^2/(1-x)}{r_-^2 - M_n^2 + i\varepsilon} \phi_n(x)\Gamma_n(y) \qquad (2.8a)$$

ii) $\underline{0 \leq x \leq 1,\ 0 \leq y \leq 1}$

The decomposition of T becomes

$$T(x,y;r^2) = \frac{ig^2}{r_-^2}\left[\frac{g^2}{\pi}\left(N - \frac{1}{N}\right)\right]^{-1} \left\{-\left(M^2 - \frac{m_i^2}{x} - \frac{m_j^2}{1-x}\right)\delta(x-y) + \left(M^2 - \frac{m_i^2}{x} - \frac{m_i^2}{1-x}\right)\left(M^2 - \frac{m_j^2}{y} - \frac{m_j^2}{1-y}\right) \sum \frac{\phi_n(x)\phi_n(y)}{r_-^2 - M_n^2 + i\varepsilon}\right\} \qquad (2.8b)$$

Given the above definitions of the scattering amplitude, we are ready to compute the Feynman diagrams that involve $q-\bar{q}$ scattering. The forms of the scattering amplitude given in Eqs.(2.8a,b) shall play a central role in the computations of the O(1/N) Feynman diagrams in Sec.IV.

III. HIGHER ORDERS IN 1/N

In this section we shall compute the 1/N corrections to the quark propagator, gluon propagator and the quark-gluon vertex. The corrections of course include all the powers of $g^2(N-1/N)$ to O(1/N).

i) Quark self energy

The leading order dressed quark propagator $S^{(0)}(p)$ has the usual expansion in terms of the bare propagator $S_0(p)$ given in Eq.(3.1) and in Fig.5a :

$$S^{(0)}(p) = S_0(p) + S_0(p)\,\tfrac{i}{2}\Sigma_0(p)\,S_0(p) + \cdots \tag{3.1}$$

where $\Sigma_0(p)$ is the quark self-energy to O(1). It satisfies the boostrap equation in Fig.5b .

To O(1/N), the self energy $\Sigma(p)$ of the quark operator

$$S(p) = \frac{i}{2}\left(p_+ + \Sigma_- - \frac{m^2 - i\varepsilon}{2p_-}\right)^{-1}$$

contains the leading order $\Sigma_0(p)$ terms and two O(1/N) corrections, $\Sigma_1(p)$, $\Sigma_2(p)$, as shown in Fig.6.

The higher order self-energy terms Σ_1 and Σ_2 are described in Fig.7. Σ_1 is a planar diagram with a quark loop in it (worm-hole). The Σ_2 term is also planar, but the quark loop now is placed on the boundary of the diagram and constitutes part of the boundary.

As shown in Fig.7, Σ_1 is obtained from Σ_2 by exchanging planar gluons between its external legs. We shall give two proofs that the Σ_1 term vanishes. First, consider the expansion of the dressed quark propagator $S(p)$ in terms of Σ_0, Σ_1 and Σ_2 as given in Fig.8. The bootstrap equation in Fig.9 follows from the expansion in Fig.8, by exchanging a single gluon at the external legs of each term (here and for the rest of the paper, we shall represent $S^{(0)}(p)$ by a bare line for simplicity, not displaying the leading order correction to it). The last two diagrams in the first line of Fig.9 add up to give Σ_1 and the boostrap equation involves only Σ_0 and Σ_1. On the other hand, the loop integral on the left-hand side of the equation gives just the leading order self-energy Σ_0

$$\frac{i}{2}\left[\Sigma_0(p) + \Sigma_1(p)\right] = -i\,\frac{4g^2}{(2\pi)^2}\left(N - \frac{1}{N}\right)\int \frac{d^2k}{(p-k)^2}\,S(k)$$

$$= \frac{i}{2}\,\Sigma_0(p) \tag{3.2}$$

In conclusion $\Sigma_1(p)$ must be zero. This result can also be anticipated from the relation between Σ_1 and Σ_2, given in Fig.7. $\Sigma_2(p)$ can be written in terms of the $q-\bar{q}$ scattering amplitude T, as shown in Fig.10.

The single gluon diagram in Fig.10 vanishes upon loop integration. The next diagram involves meson intermediate states. It is the familiar one-loop renormalization diagram and will eventually become the only O(1/N) quark self-energy correction. Let us consider $\Sigma_2(p)$ with a single gluon exchange between its legs, as shown in Fig.11. It is the second term contained in $\Sigma_1(p)$ in Fig.10 and is given by

$$i\,\frac{\pi}{N}\,\frac{16\,g^2}{(2\pi)^4}\sum_n \int \frac{d^2k}{(p-k)^2}\int \frac{d^2r}{r^2}\,S(k)\,\frac{\Gamma_n^2(k,r)}{r^2 - M_n^2 + i\varepsilon}\,S(k-r)S(k) \tag{3.3a}$$

The terms relevant to k_+ and r_+ integration are

$$\int dk_+ \left(k_+ - r_+ - \frac{m_b^2 - i\varepsilon}{2(k_- - r_-)}\right)^{-1}\left(k_+ - \frac{m_a^2 - i\varepsilon}{2k_-}\right)^{-2} =$$

$$= 2\pi i \left[\frac{\theta(k_-)\,\theta(r_- - k_-)}{\left(r_+ - \frac{m_a^2}{2k_-} - \frac{m_b^2}{2(r_- - k_-)} + i\varepsilon\right)^2} - \frac{\theta(-k_-)\,\theta(k_- - r_-)}{\left(r_+ - \frac{m_a^2}{2k_-} - \frac{m_b^2}{2(r_- - k_-)} - i\varepsilon\right)^2}\right] \tag{3.3b}$$

and

$$\int dr_+ \left[\frac{\theta(r_-)\,\theta(k_-)\,\theta(r_- - k_-)}{\left(r_+ - \frac{M_a^2}{2r_-} + i\varepsilon\right)\left(r_+ - \frac{m_a^2}{2k_-} - \frac{m_b^2}{2(r_- - k_-)} + i\varepsilon\right)^2}\right.$$

$$\left. - \frac{\theta(-r_-)\,\theta(-k_-)\,\theta(k_- - r_-)}{\left(r_+ - \frac{M_a^2}{2r_-} - i\varepsilon\right)\left(r_+ - \frac{m_a^2}{2k_-} - \frac{m_b^2}{2(r_- - k_-)} - i\varepsilon\right)^2}\right] = 0 \tag{3.3c}$$

The r_+ integral always has the poles in the same half plane and the result is zero. With this observation, we see that the remaining terms of $\Sigma_1(p)$ must also vanish.

The surviving O(1/N) quark self energy is the non-zero part of $\Sigma_2(p)$ in Fig.10 :

$$\frac{i}{2}\Sigma_2(p) = \frac{1}{N}\sum_n \int \frac{dr_-}{2r_-^3}\left[\frac{\theta(r_-)\,\theta(p_- - r_-)}{p_+ - \frac{M_n^2}{2r_-} - \frac{m_a^2}{2(p_- - r_-)} + i\varepsilon}\right.$$

$$\left. + \frac{\theta(-r_-)\,\theta(r_- - p_-)}{p_+ - \frac{M_n^2}{2r_-} - \frac{m_a^2}{2(p_- - r_-)} + i\varepsilon}\right] \Gamma_n^2(p_-/r_-) \tag{3.4}$$

$\Sigma_2(p)$ is in general different from zero. With the singular cut-off, it would have become zero. Quark mass is not a gauge invariant quantity hence different regularization schemes yield different results for $\Sigma(p)$.

ii) Gluon self energy

The gluon self energy to O(1/N) is given by the diagram of Fig.12. The gluon dressed propagator $D(p)$ is expanded in terms of the bare propagator $D_0(p)$ and the self-energy $\pi(p)$ as

$$\mathcal{D}(p) = \frac{i}{k^2 + \Pi(k)} = D_0(k) + D_0(k)\,i\Pi(k)\,D_0(k) + \cdots \tag{3.5}$$

where $\pi(p)$ is given by

$$i\Pi(p) = -\frac{g^2}{(2\pi)^2}\int d^2k\; S(k)S(p+k) \tag{3.6}$$

iii) Vertex renormalization

The corrections to the quark-gluon coupling to O(1/N) arise from the diagrams in Fig.13. The evaluation of Fig.13 gives for the renormalized coupling constant g_R

$$g_R = g\left\{1 + \frac{4\pi}{N}\frac{1}{(2\pi)^2}\sum_n \int \frac{d^2r}{r^2}\,\frac{\Gamma_n(p_-/r_-)\,\Gamma_n(q_-/r_-)}{r^2 - M_n^2 + i\varepsilon}\,S(p-r)S(q-r)\right\} \tag{3.7}$$

Thus, we see that the quark and gluon self energies and the vertex correction do not vanish to O(1/N) by themselves, as in the case of singular cut-off scheme. As will be shown in Sec.IV for the meson bound state equation however, there exists a remarkable internal cancellation mechanism for those corrections within a given process.

IV. MESON BOUND STATE EQUATION TO ORDER 1/N

We now consider the 1/N corrections to the meson mass operator. The meson bound state wave function, when the next-to-leading order terms are included, satisfies the Bethe-Salpeter equation given in Fig.14. The first term in Fig.14 is the leading order single gluon exchange diagram. The second and third terms are the O(1/N) mass corrections to the quark propagators. The fourth term is the well-known [1] s-channel "worm-hole"

correction to the planar gluon exchange diagram. The fifth term involves t-channel exchanges and shall contribute only for equal quark masses. Finally the non-planar two-gluon exchange diagram of the sixth term also contributes in the case of equal quark masses. The mass correction terms were considered in Sec.III. Now, we study the remaining fourth, fifth and the sixth diagrams of Fig.14 in detail.

With the usual decomposition (Fig.4) of the T-matrix shown in Fig.14, the single quark loop diagram of the fourth term contains the gluon self-energy and vertex corrections in addition to the two-meson intermediate state diagram.

Having performed the plus-momentum integrals (with the bound state condition $0 \leq p_- \leq r_-$) for this one-loop term, we obtain four types of diagrams, differing according to the values of quark momenta entering and leaving each T matrix of the diagram. With the labelling of momenta given in Fig.15, we have the following θ-function combination common to all of the diagram types:

$$\theta(q_-)\,\theta(r_- - q_-)\,\theta(r_-')\,\theta(r_- - r_-')\,\theta(p_-)\,\theta(r_- - p_-) \tag{4.1}$$

The diagram types, according to the remaining two θ-functions, are

i) $\underline{\theta(q_- - r_-')\theta(p_- - r_-')}$

In the upper T matrix, the condition in Eq.(2.8b) is satisfied, hence we can use the corresponding decomposition given there. This decomposition is shown in Fig.16a. The first disconnected piece in Fig.16a cancels the 1/N correction to the upper quark propagator of the meson bound state. The lower vertices are meson wave functions, whereas the upper T matrix is still to be computed in its usual form with the proper $q\text{-}\bar{q}$ meson vertex functions.

ii) $\underline{\theta(r_-' - q_-)\theta(r_-' - p_-)}$

This one is similar to the type i) diagram and the disconnected piece now cancels the 1/N correction to the lower quark propagator, as shown in Fig.16b .

iii) $\underline{\theta(q_- - r_-')\theta(r_-' - r_-)}$

In this case one quark momentum in each T-matrix satisfies the condition in Eq.(2.8a).for which the corresponding T-matrix decomposition is shown in Fig.16c.

iv) $\underline{\theta(r_-' - q_-)\theta(r_- - r_-')}$

This diagram is similar to type iii), as shown in Fig.16d.

The diagrams of Figs.16c,d are responsible for the cancellation of the gluon self energy and vertex corrections that appear in the usual expansions of the T-matrices of Fig.16 according to Fig.4. To see this, consider the detailed reduction of the diagram in Fig.16c, given in Figs.17a,b,c. In Fig.17a, the upper T-matrix is decomposed as usual, where the first diagram contains the gluon self-energy and lower vertex correction pieces.

Using Eq.(2.8a) we obtain the expansion given in Fig.17b for the second term in Fig.17a. The first term in Fig.17b cancels against the first term in Fig.17b. Now we repeat the same reduction for the lower T-matrix in Fig.17b and obtain the expression in Fig.17c when $1 \gg q_- \gg r_-' \gg p_- \gg 0$. The above observations explicitly show how the gluon and vertex corrections, which were formally present, are removed from the picture.

We would like to stress that the non-renormalization of the quark and gluon propagators and the gluon-quark coupling constant follows from the fact that there is always a pair of internal quark momenta satisfying the conditions in Eqs.(2.8a,b), which enabled us to rewrite the T matrices in terms of the intermediate meson wave functions instead of the proper vertices.

Now we present the contributions of the diagrams in Fig.s17a,b,c to the "potential part" of the Bethe-Salpeter equation satisfied by the meson bound state $\phi(x)$ of mass M. In the lowest order that equation reads [1),8)]

$$\left(M^2 - \frac{m_i^2}{x} - \frac{m_j^2}{1-x}\right)\phi(x) = -\frac{g^2}{\pi}\left(N - \frac{1}{N}\right)\int_0^1 \frac{dy}{(y-x)^2}\,\phi(y) \tag{4.2}$$

Diagrams (i and iv) contribute to the right-hand side of Eq.(4.2) the quantity

$$\frac{g^2}{\pi}\sum_{n,m}\int \frac{dz}{z^2(1-z)}\left(M^2 - \frac{M_n^2}{1-z} - \frac{M_m^2}{z}\right)^{-1}\int\!\!\int \frac{dy\,dt}{(y-t)^2}\left[\phi(y) - \phi(t)\right]\cdot$$

$$\cdot\ \phi_n\left(\frac{t}{z}\right)\Gamma_n\left(\frac{x}{z}\right)\phi_m\left(\frac{y-z}{1-z}\right)\phi_m\left(\frac{x-z}{1-z}\right) \tag{4.3}$$

The contribution of (ii and iii) is

$$-\frac{g^2}{\pi}\sum_{n,m}\int\frac{dz}{z(1-z)^2}\left(M^2-\frac{M_n^2}{1-z}-\frac{M_m^2}{z}\right)^{-1}\iint\frac{dy\,dt}{(y-t)^2}[\phi(y)-\phi(t)]$$
$$\otimes\,\phi_n\left(\frac{t}{z}\right)\phi_n\left(\frac{x}{z}\right)\phi_m\left(\frac{y-z}{1-z}\right)\Gamma_m\left(\frac{x-z}{1-z}\right) \qquad (4.4)$$

In Eqs.(4.3) and (4.4) we have used the expression Eq.(2.5) for one of the proper vertices in the integrands in order to make the results more transparent for the discussion of the zero mass bound state, given in Sec.V. The integration limits in Eqs.(4.3) and (4.4) and in other equations, follow directly from the arguments of the wave functions which must lie in the interval (0,1) and/or from the positivity of the explicit mass terms.

The fifth and sixth diagrams in Fig.14 contribute when the quark masses are equal. The fifth diagram has planar gluon exchanges between the internal and external quark lines where the gluon exchange diagrams are pair creation annihilation interactions, as shown in Figs.18a,b. In Fig.19 the T-matrix of the fifth diagram in Fig.14 is decomposed according to Fig.4. The single gluon exchange diagram in Fig.19 gives

$$-\frac{1}{2}\lambda^{\kappa}_{ij}\lambda^{\kappa}_{ji}\frac{g^2}{\pi}\int_0^1 dy\,\phi(y) \qquad (4.5)$$

This vanishes when the colour group is SU(N). However, the multiple gluon exchanges in Fig.18 survive the colour index summations and lead to the t-channel intermediate meson state of the second diagram in Fig.19. Depending on the sign of the momentum of the intermediate states, we have two cases for this diagram, in which the intermediate state is always a right moving meson.

i) $\underline{q-p>0}$

This case is shown in Fig.20a. The contribution to the Bethe-Salpeter equation is

$$\frac{g^2}{\pi}\frac{g^2}{\pi}\left(N-\frac{1}{N}\right)\sum_n\int\frac{dy}{y-x}\int\frac{dz}{(z-y)^2}\int\frac{dt}{(t+y-1)^2}\frac{\phi_n\left(\frac{z}{y-z}\right)\phi_n\left(\frac{t}{y-z}\right)}{M^2-\frac{m^2}{x}-\frac{m^2}{1-y}-\frac{M_n^2}{y-x}}\phi(y) \qquad (4.6a)$$

ii) $\underline{p-q>0}$

In this case, the t-channel contribution becomes

$$\frac{g^2}{\pi}\frac{g^2}{\pi}\left(N-\frac{1}{N}\right)\sum_n\int\frac{dy}{x-y}\int\frac{dz}{(z-y)^2}\int\frac{dt}{(t+x-1)^2}\frac{\phi_n\left(\frac{z}{x-y}\right)\phi_n\left(\frac{t}{x-y}\right)}{M^2-\frac{m^2}{y}-\frac{m^2}{1-x}-\frac{M_n^2}{x-y}}\phi(y) \qquad (4.6b)$$

The sixth diagram in Fig.14, though not planar, is also $O(1/N)$, because of a closed colour loop (Fig.21). Again we have two cases defined by the functions of momenta.

i) $\underline{\theta(p-k-r)\theta(q+k)}$

The result of this case is

$$\frac{g^2}{\pi}\frac{g^2}{\pi}\left(N-\frac{1}{N}\right)\iint\frac{dy\,dz}{z^2(1-z)^2}\frac{\phi(y)}{M^2-\frac{m^2}{1-y}-\frac{m^2}{y-z}-\frac{m^2}{x+z-1}-\frac{m^2}{1-x}} \qquad (4.7a)$$

ii) $\underline{\theta(r+k-p)\,\theta(-q-k)}$

The contribution is

$$\frac{g^2}{\pi}\frac{g^2}{\pi}\left(N-\frac{1}{N}\right)\int\int\int\frac{dz}{z^2(1-z)^2}\frac{\phi(y)}{M^2-\frac{m^2}{z-y}-\frac{m^2}{x}-\frac{m^2}{y}-\frac{m^2}{1-x-z}} \qquad (4.7b)$$

Note that the diagram in Fig.21 can be viewed as a planar quark-quark scattering diagram if we twist the external quark legs. If we were to consider the twisted diagram together with its counterparts in all orders in 1/N, we would obtain the set of diargams shown in Fig.22, where their 1/N orders are also indicated.

The planar q-q diagrams (or the twisted gluon diagrams of $q-\bar{q}$ scattering) in Fig.22, when summed to all orders, can add up to give rise to quark-quark intermediate states. Such a bound state which is in general colour non-singlet would contribute to the meson equation as shown in Fig.23. It should be noted that a diagram like that in Fig.21 is O(1/N).

There already exists such a colour antisymmetric bound state of diquarks which satifies the Bethe-Salepter equation shown in Fig.24 [9]. In a recent detailed study [10] of the quark-quark scattering and the baryon and baryonium states [11], we show that the last two diagrams in Fig.14 can in fact be obtained by inserting the quark-quark scattering amplitude T_{qq} given in Fig.25 in the meson Bethe-Salpeter equation, in the manner shown in Fig.26.

The qq scattering amplitude to O(1/N) consists of the single gluon and single meson intermediate state diagrams; the first three diagrams in Fig.25. The fourth diagram contains the above-mentioned antisymmetric diquark intermediate states(obtained in the leading order, by the first three terms in T_{qq}) and is O(1/N) since the proper diquark-quark vertex is O(1/N). We have also included the two-meson intermediate state diagram in Fig.25 as another example of $O(1/N^2)$ terms. As shown in Fig.25, this diagram's contribution remains $O(1/N^2)$ where the contribution of the diquark diagram becomes O(1/N), the same as the other $q-\bar{q}$ intermediate states of that order. For completeness, we present the diquark intermediate state contributing to the meson equation, since this contribution effectively replaces the two-gluon contributions in Eq.(4.7)

$$(N_{-1})\sum_n \left\{ \int_{1-x}^{1} \frac{dy}{(y+x-1)^3} \frac{D_n\left(\frac{y}{y+x-1}\right) D_n\left(\frac{1-y}{y+x-1}\right)}{M^2 - \frac{m^2}{1-y} - \frac{m^2}{1-x} - \frac{M_n^2}{y+x-1}} + \int_0^{1-x} \frac{dy}{(1-x-y)^3} \frac{D_n\left(\frac{y}{1-x-y}\right) D_n\left(\frac{1-y}{1-x-y}\right)}{M^2 - \frac{m^2}{y} - \frac{m^2}{x} - \frac{M_n^2}{1-x-y}} \right\} \tag{4.8}$$

where D_n is the diquark-quark paper vertex [9]. Therefore we observe that the qq intermediate states start to mix with the $q\bar{q}$ intermediate states in the next-to-leading O(1/N) order in $q-\bar{q}$ scattering through t-channel processes, a feature which of course could not be surmised in the leading order.

V. ON THE ZERO MASS BOSON

The leading order meson equation is known to possess a zero-mass solution in the chiral limit [1]

$$\phi_0(x) = \theta(x)\theta(1-x) \tag{5.1}$$

Similar massless solutions also exist for some baryon and baryonium models [10],[11].

According to a theorem by Coleman [7], the spontaneous breaking of a continuous symmetry in two dimensions is not possible and there are no Goldstone bosons. Thus the question of persistance of such a state in higher orders is a question of extreme importance, and was recently reconsidered [12]. Below we present a brief summary of our results on the problem, which is a by-product of our general treatment of next-to-leading corrections.

Let us consider the interaction Hamiltonian diagrams in Fig.27, which are, in the order they appear, the particle non-conserving diagrams and the pair creation-annihilation diagram.

The three meson vertex in Fig.28 contains the first and second terms of Fig.27. When the decaying meson ϕ_1 is the massless ϕ_0 state of Eq.(5.1), this vertex vanishes [13]. In fact, when acting on the massless state in the manner shown in Fig.28, the particle non-conserving interaction diagram set always annihilates that state [12], which is also confirmed by our results in Eqs.(4.3) and (4.4). In summary, the equation for ϕ_0 does not get any contribution from the one loop diagram (the fourth terms) in Fig.14.

The last two diagrams in Fig.14, on the other hand, shall have, in general, non-zero contributions to the ϕ_0 meson equation to O(1/N), since there is no obvious reason for the results in Eqs.(4.6a), (4.6b), (4.7a) and (4.7b) to vanish for that state. With the non-zero contributions of the t-channel and the crossed gluon diagrams the O(1/N) meson equation is no longer

satisfied by $\phi_0(x)$ when $m_b = 0$, $M_0 = 0$ and we conclude that the massless boson gains a mass as a result of the inclusion of the higher order corrections. Let us remind ourselves that a similar phenomenon takes place in the Gross-Neveu model; namely the "Goldstone boson" which exists in the leading order is shown to disappear in higher orders in 1/n, where n is the number of the components of the fermion field [14]. Details of the proof is given elsewhere [15].

VI. CONCLUDING REMARKS

The main aim of this work was to study the 1/N corrections to the meson equation in regular cutt-off scheme. This problem proved to be a rather illuminating example to demonstrate that physical results should be independent of the infra-red regularization scheme, we have observed that the quark and gluon self energies and the vertex corrections do not vanish to $O(1/N)$ by themselves as in the case of the λ cut-off scheme, but there exists a remarkable internal cancellation mechanism for these corrections within a given physical process, in our case the meson mass operator.

We have demonstrated that there are important new contributions to the meson mass in the 1/N order. In addition to the worm-hole correction to the planar limit [2] (which is an s-channel diagram with two intermediate meson states), there are t-channel meson exchange diagrams, and the crossed gluon diagram which contribute in the equal quark mass limit. The crossed gluon diagram is shown to lead to a t-channel diagram, with an intermediate quark-quark bound state when this diagram is considered to all orders in 1/N. Thus qq intermediate states begin to mix with the $q\bar{q}$ intermediate states in the 1/N order in $q\bar{q}$ scattering through t-channel processes, a feature which of course could not be surmised in the leading order. These new effects would contribute to the imaginary parts of the mass operator also, thus modifying the old width computations [5]. Work in this direction is in progress.

The most striking by-product of the new effects we discovered is the elimination of the leading order zero-mass boson in the 1/N order, in agreement with Coleman's theorem.

In summary our analysis shows that to order 1/N, QCD_2 again can be described by an effective theory of hadrons (in addition to ordinary $q\bar{q}$ mesons, there are new qq hadrons, which dominate the t-channel diagrams) with no quarks and gluons.

ACKNOWLEDGMENTS

We are grateful to S. Kaptanoğlu for enjoyable discussions, and Professor N.S. Craigie for reading the manuscript and for a useful comment. We would like to thank Professor Abdus Salam, the International Atomic Energy Agency and UNESCO for hospitality at the International Centre for Theoretical Physics, Trieste, where this work was completed. We also thank TUBITAK, the Scientific and Technical Research Council of Turkey, for financial support.

REFERENCES

1) G. 't Hooft, Nucl. Phys. B75, 461 (1974); ibid. B72, 461 (1974).

2) C. Callan, N. Coote and D. Gross, Phys. Rev. D13, 1649 (1976).

3) M. Einhorn, Phys. Rev. D14, 2451 (1976).

4) E. Witten, Nucl. Phys. B160, 57 (1979).

5) R.C. Brown, J. Ellis, M. Schmidt and J. Weiss, Nucl. Phys. B128, 131 (1977).

6) Y. Frishman, Nucl. Phys. B148, 74 (1979).

7) S. Coleman, Commun. Math. Phys. 31, 259 (1973).

8) N.K. Pak and H.C. Tze, Phys. Rev. D14, 3472 (1976).

9) V. Pervushin and D. Ebert, Theor. Math. Phys. 36, 759 (1978).

10) M. Durgut and N.K. Pak, "Quark-quark scattering baryons and baryonium in QCD_2",ICTP, Trieste, in preparation.

11) M. Durgut, Nucl. Phys. B116, 223 (1976);
See also Ph.D. Thesis, Stony Brook (1979).

12) D. Amati and E. Rabinovici, Phys. Letters 101B, 407 (1981);
W. Buchmuller, S. Love and R. Peccei, MPI-PAE/PTh-70/81;
S. Elitzur, R. Frishman and E. Rabinovich, CERN TH-2137, August 1981.

13) I. Bars, Nucl. Phys. B111, 413 (1976).

14) D. Gross and A. Neveu, Phys. Rev. D10, 3235 (1974).

15) M. Durgut and N.K. Pak, "On the zero mass boson in QCD_2", Middle East Technical University report, June 1982.

FIGURE CAPTIONS

Fig.1 Effective Feynman rules

Fig.2 $q\bar{q}$ scattering amplitude edquations.

Fig.3 Meson-quark antiquark vertex

Fig.4 Leading order $q\bar{q}$ scattering diagrams

Fig.5a Leading order quark propagator

Fig.5b Leading order quark self-energy equation.

Fig.6 Quark self-energy expansion

Fig.7 O(1/N) quark self-energy terms

Fig.8 Dressed quark propagator

Fig.9 Bootstrap equation for $\Sigma(p)$

Fig.10 Σ_2 term

Fig.11 Contribution of Σ_2 to Fig.9

Fig.12 Gluon self energy

Fig.13 Vertex renormalization

Fig.14 Bethe-Salpeter equation for the meson state

Fig.15 The worm hole diagram

Fig.16a Diagram of type i

Fig.16b Diagram of type ii

Fig.16c Diagram of type iii

Fig.16d Diagram of type iv

Fig.17a Type ii diagram with $\Gamma_n\Gamma_n$ vertices

Fig.17b Type ii diagram with $\Gamma_n\phi_n$ vertices

Fig.17c Fully reduced type ii diagram

Fig.18a Single pair creation annihilation

Fig.18b Multiple pair creation annihilation

Fig.19 The fifth diagram in Fig.14

Fig.20a t channel diagram for case i

Fig.20b t channel diagram for case ii

Fig.21 Non-planar contribution to Fig.14

Fig.22 Effective quark-quark scattering in meson equation

Fig.23 Diquark intermediate state.

Fig.24 Diquark bound state equation

Fig.25 Quark quark scattering amplitude

Fig.26 Quark-quark scattering contribution

Fig.27 Interaction Hamiltonian term

Fig.28 Three meson vertex to leading order

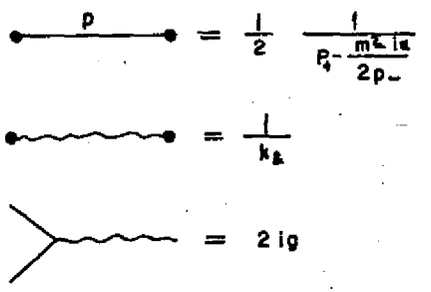

Fig. 1

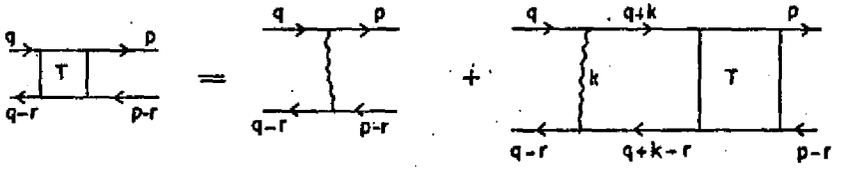

Fig. 2

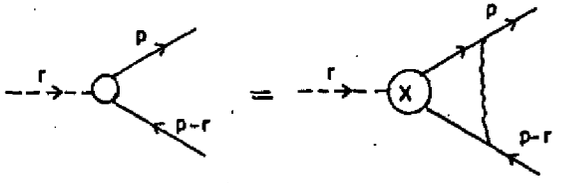

Fig. 3

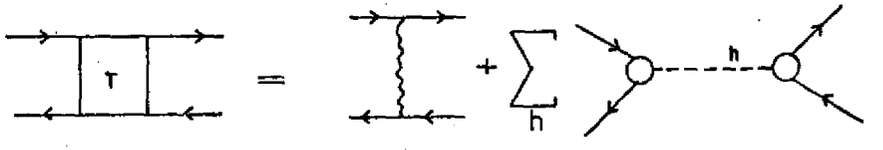

Fig. 4

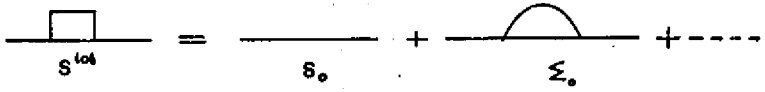

Fig. 5.a

Fig. 5.b

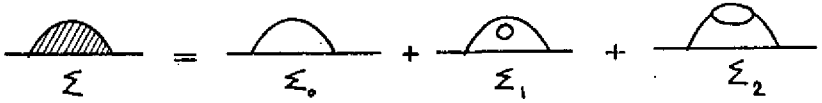

Fig. 6

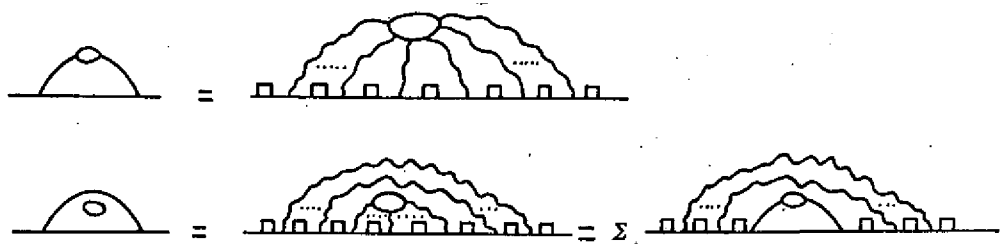

Fig.7

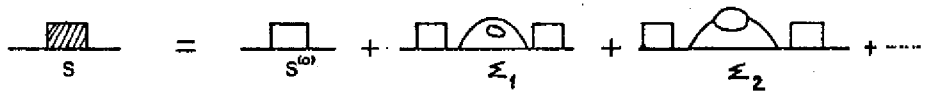

Fig. 8

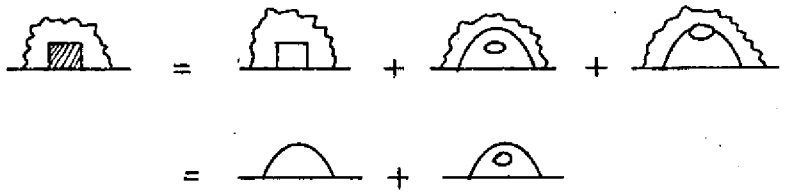

Fig. 9

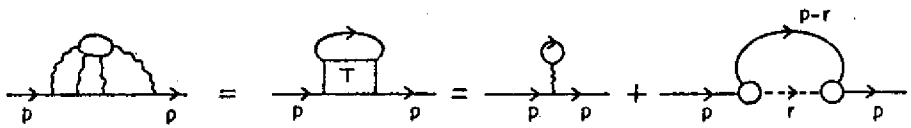

Fig.10

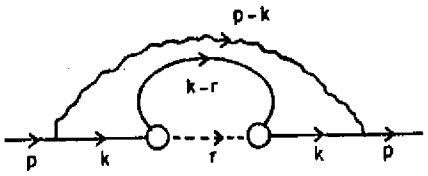

Fig. 11

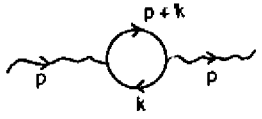

Fig. 12

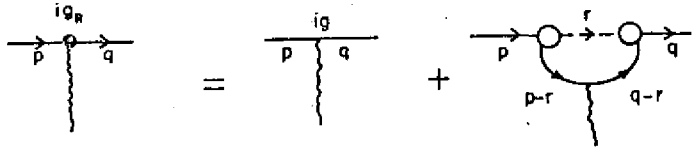

Fig. 13

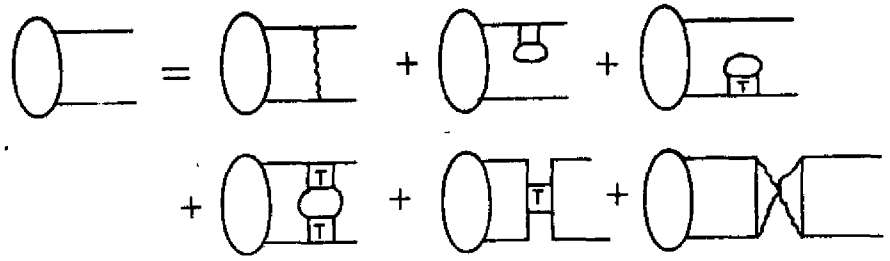

Fig. 14

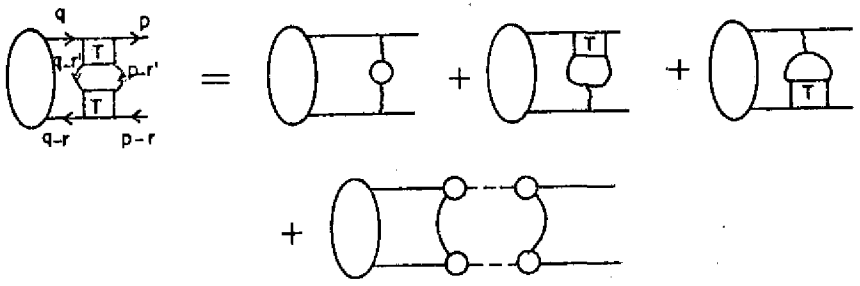

Fig. 15

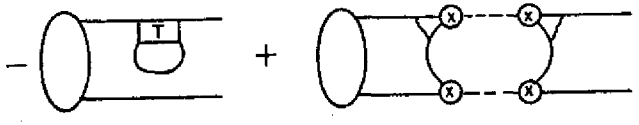

Fig. 16 a

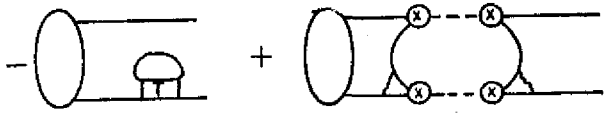

Fig. 16 b

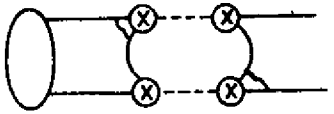

Fig. 16. c

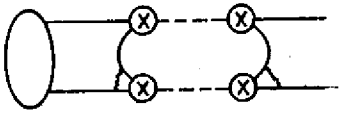

Fig. 16. d

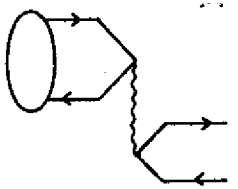

Fig. 18.a

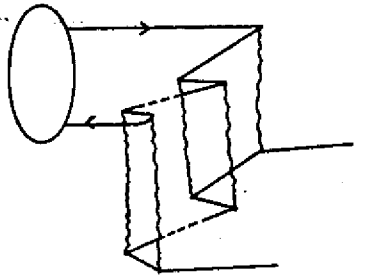

Fig. 18.b

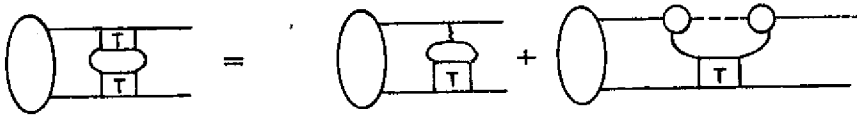

Fig.17 . a

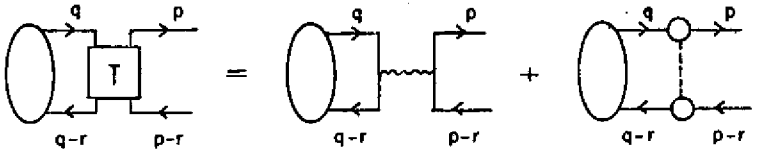

Fig. 19

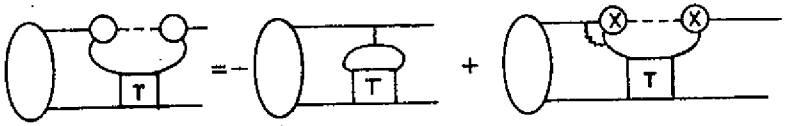

Fig.17. b

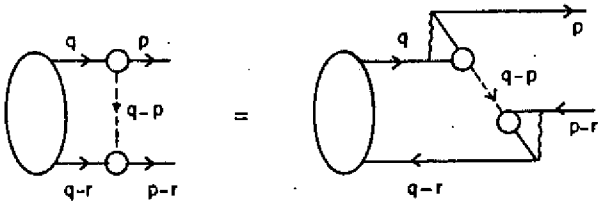

Fig.20. a

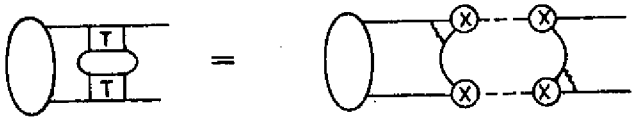

Fig. 17. c

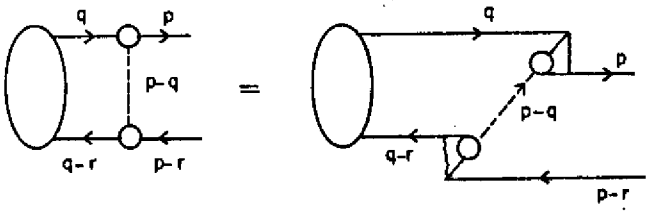

Fig. 20. b

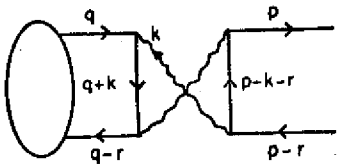

Fig. 21

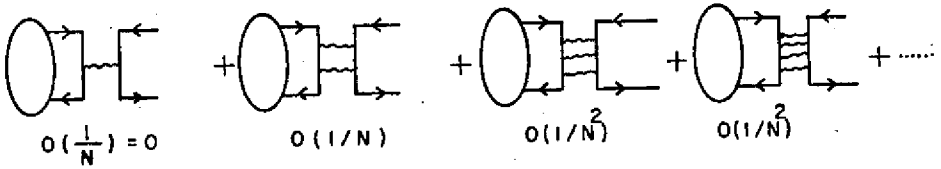

Fig. 22

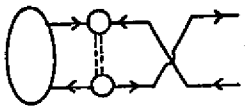

Fig. 23

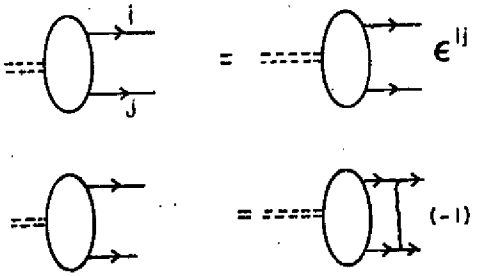

Fig. 24

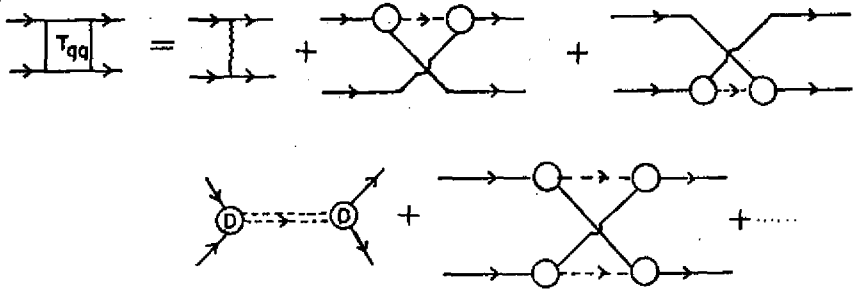

Fig. 25. Quark - Quark Scattering Amplitude

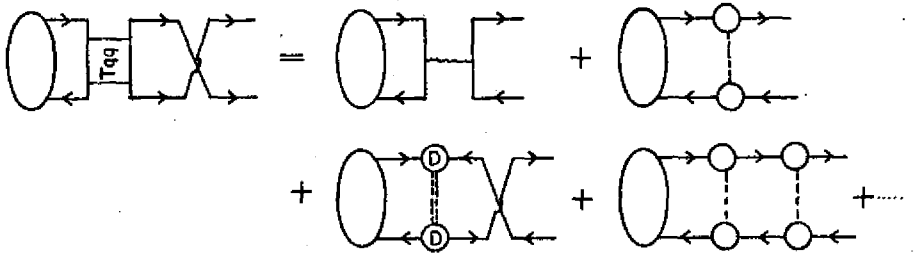

Fig. 26 . Quark— Quark Scattering Contributions

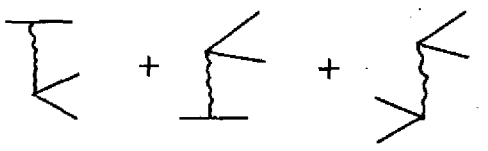

Fig. 27

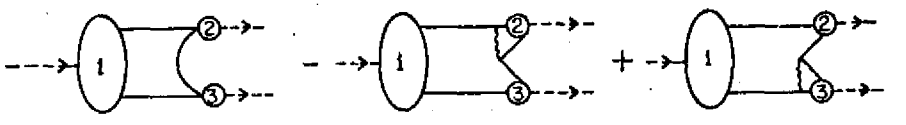

Fig. 28

CURRENT ICTP PUBLICATIONS AND INTERNAL REPORTS

IC/82/23 INT.REP.* — SUN KUN OH - Mass splitting between B^+ and B^0 mesons.

IC/82/24 INT.REP.* — A. BREZINI - Self-consistent study of localization near band edges.

IC/82/25 INT.REP.* — C. PANAGIOTAKOPOULOS - Dirac monopoles and non-Abelian gauge theories.

IC/82/26 — CAO CHANG-qi and DING XING-fu - Intermediate symmetry $SU(4)_{EC} \times SU(2)_L \times U(1)_Y$ and the SU(N) unification series.

IC/82/27 — H.B. GHASSIB and S. CHATTERJEE - ^{4}He-impurity effects on normal liquid ^{3}He at low temperatures - I: Preliminary ideas and calculations.

IC/82/28 — C. PANAGIOTAKOPOULOS, ABDUS SALAM and J. STRATHDEE - Supersymmetric local field theory of monopoles.

IC/82/29 INT.REP.* — G.A. CHRISTOS - Concerning the proofs of spontaneous chiral symmetry breaking in QCD from the effective Lagrangian point of view.

IC/82/30 INT.REP.* — M.I. YOUSEF - Diffraction model analyses of polarized ^{6}Li elastic scattering.

IC/82/31 — L. MIZRACHI - Electric-magnetic duality in non-Abelian gauge theories.

IC/82/32 INT.REP.* — W. MECKLENBURG - Hierarchial spontaneous compactification.

IC/82/33 — C. PANAGIOTAKOPOULOS - Infinity subtraction in a quantum field theory of charges and monopoles.

IC/82/34 INT.REP.* — M.W. KALINOWSKI, M. SEWERYNSKI and L. SZYMANOWSKI - On the F equation.

IC/82/35 INT.REP.* — H.C. LEE, LI BING-AN, SHEN QI-XING, ZHANG MEI-MAN and YU HONG - Electroweak interference effects in the high energy $e^+ + e^- \rightarrow e^+ + e^-$ + hadrons process.

IC/82/36 — G.A. CHRISTOS - Some aspects of the U(1) problem and the pseudoscalar mass spectrum.

IC/82/37 — C. MUKKU - Gauge theories in hot environments: Fermion contributions to one-loop.

IC/82/38 INT.REP.* — W. KOTARSKI and A. KOWALEWSKI - Optimal control of distributed parameter system with incomplete information about the initial condition.

IC/82/39 INT.REP.* — M.I. YOUSEF - Diffraction model analysis of polarized triton and ^{3}He elastic scattering.

IC/82/40 INT.REP.* — S. SELZER and N. MAJLIS - Effects of surface exchange anisotropy in Heisenberg ferromagnetic insulators.

IC/82/41 INT.REP.* — H.R. HAROON - Subcritical assemblies, use and their feasibility assessment.

IC/82/42 — W. ANDREONI and M.P. TOSI - Why is AgBr not a superionic conductor?

THESE PREPRINTS ARE AVAILABLE FROM THE PUBLICATIONS OFFICE, ICTP, P.O. BOX 586, I-34100 TRIESTE, ITALY.

IC/82/43 — N.S. CRAIGIE and J. STERN - What can we learn from sum rules for vertex functions in QCD?

IC/82/44 INT.REP.* — ERNEST C. NJAU - Distortions in power spectra of digitised signals - I: General formulations.

IC/82/45 INT.REP.* — ERNEST C. NJAU - Distortions in power spectra of digitised signals - II: Suggested solution.

IC/82/46 INT.REP.* — H.R. DALAFI - A critique of nuclear behaviour at high angular momentum.

IC/82/47 — N.S. CRAIGIE and P. RATCLIFFE - Higher power QCD mechanisms for large p_T strange or charmed baryon production in polarized proton-proton collisions.

IC/82/48 INT.REP.* — B.R. BULKA - Electron density of states in a one-dimensional distorted system with impurities: Coherent potential approximation.

IC/82/49 INT.REP.* — J. GORECKI - On the resistivity of metal-tellurium alloys for low concentrations of tellurium.

IC/82/50 — S. RANDJBAR-DAEMI and R. PERCACCI - Spontaneous compactification of a (4+d)-dimensional Kaluza-Klein theory into $M_4 \times G/H$ for arbitrary G and H.

IC/82/51 INT.REP.* — P.S. CHEE - On the extension of H^P-functions in polydiscs.

IC/82/53 INT.REP.* — S. YOKSAN - Critical temperature of two-band superconductors containing Kondo impurities.

IC/82/54 — M. ÖZER - More on generalized gauge hierarchies.

IC/82/55 — N.S. CRAIGIE and P. RATCLIFFE - A simple method for isolating order α_S and α_S^2 corrections from polarized deep-inelastic scattering data.

IC/82/56 — C. PANAGIOTAKOPOULOS - Renormalization of the QEMD of a dyon field.

IC/82/57 INT.REP.* — J.A. MAGPANTAY - Towards an effective bilocal theory from QCD in a background.

IC/82/58 — S. CHAKRABARTI - On stability domain of stationary solitons in a many-charge field model with non-Abelian internal symmetry.

IC/82/59 INT.REP.* — J.K. ABOAYE and D.S. PAYIDA - High temperature internal friction in pure aluminium.

IC/82/60 — Y. FUJIMOTO and ZHAO ZHIYONG - N-$\bar{N}$ oscillation in SO(10) and SU(6) supersymmetric grand unified models.

IC/82/61 — J. GORECKI and J. POPIELAWSKI - On the application of the long mean free path approximation to the theory of electron transport properties in liquid noble metals.

IC/82/62 — I.M. REDA, J. HAFNER, P. PONGRATZ, A. WAGENDRISTEL, H. BANGERT and P.K. BHAT - Amorphous Cu-Ag films with high stability.

IC/PD/82/1 INT.REP. — PHYSICS AND DEVELOPMENT (Winter College on Nuclear Physics and Reactors, 25 January - 19 March 1982).